

Luminescence and scintillation characteristics of heavily Pr³⁺-doped PbWO₄ single crystals

M. Nikl,^{1,a)} P. Bohacek,¹ A. Vedda,² M. Fasoli,² Jan Pejchal,¹ A. Beitlerova,¹ M. Fraternali,³ and M. Livan³

¹*Institute of Physics, AS CR, Cukrovarnicka 10, 162 53 Prague, Czech Republic*

²*Department of Materials Science, University of Milano-Bicocca, Via Cozzi 53, 20125 Milan, Italy*

³*INFN, Sezione di Pavia and Dipartimento di Fisica Nucleare e Teorica, Università di Pavia, Via Bassi 5, 27100 Pavia, Italy*

(Received 21 May 2008; accepted 13 September 2008; published online 6 November 2008)

PbWO₄ single crystals with praseodymium doping in a wide concentration range (0.1–5 at % in the melt) were grown by Czochralski method. Absorption, luminescence, and scintillation characteristics were measured at room temperature. Similar to other trivalent dopants, heavy Pr³⁺ doping on one hand suppresses intrinsic host scintillation. On the other hand though, in the scintillation decay it introduces components with characteristic decay times within 500–2000 ns based on Pr³⁺ 4*f*-4*f* emission lines in the green-red part of the spectra. We discuss the suitability of such material for dual scintillation/Cherenkov light detector. © 2008 American Institute of Physics. [DOI: 10.1063/1.3008002]

I. INTRODUCTION

Single crystals of PbWO₄ (PWO) were the subject of increased interest for scintillation detection in the early 1990s because of their potential use in electromagnetic calorimeter detectors used in high energy physics accelerators. Essential luminescence characteristics of PWO had already been studied in the 1970s (Refs. 1 and 2) and the growth of tungstate and molybdate single crystals was also reported.³ However, the first systematic scintillation-oriented reports showing favorable characteristics of PWO for the above-mentioned applications^{4,5} appeared only in 1992 until 1993. An intense effort to optimize the PbWO₄ scintillator, especially with respect to its radiation hardness, resulted in finding a positive role of doping by selected stable trivalent ions (La, Y, Gd, Lu) in 1997 (see Refs. 6 and 7). Therefore Y-doping at the level of about 100 ppm has later been used for industrial production of full-size crystals (for an overview, see Refs. 8 and 9). Interestingly, some of these trivalent ions could be incorporated into the PWO host in surprisingly large concentrations of up to several percent while maintaining high structural quality and radiation hardness of the crystal. In such crystals the intrinsic blue luminescence was efficiently suppressed, and some authors proposed to use them as Cherenkov radiators.¹⁰ Others proposed¹¹ that a Coulombic compensation of their trivalent-dopant-excess charge is realized as a self-compensation process with part of the La ions residing at the W site. The same authors alternatively considered the introduction of interstitial oxygen ions.¹² Recent theoretical calculations are consistent with the latter possibility.¹³

Recently, it was demonstrated that materials that produce both scintillation and Cherenkov light could make excellent

detectors for particle physics experiments.^{14(a)} Ideally, such materials should provide scintillation and Cherenkov light of *comparable intensity with good spectral and temporal separation*. In other words, low intensity scintillation in the red part of the spectrum with a time response of the order of hundreds of nanoseconds is desired.

The Dual REAdout Module (DREAM) Collaboration tested PWO and Bi₄Ge₃O₁₂ (BGO) crystals^{14(b),14(c)} for this purpose and showed that BGO is more favorable for this application respect to pure PWO because

- (1) the BGO light yield for the scintillation component is 100 times larger than the Cherenkov one but the spectra of the two types of light are different and with the use of an optical filter one can obtain clean signals of comparable intensity and
- (2) the 300 ns scintillation decay time of BGO allows to separate easily the Cherenkov and scintillation components on the basis of the time structure of the (filtered) signals.

The aim of this work is to look for an even better suited type of crystal that could alter both the emission spectrum and the decay time of pure PWO optimizing the separation in terms of spectrum and time structure of the signals while producing comparable amounts of scintillation and Cherenkov light. Specifically, we consider Pr-doped PWO as a candidate for dual scintillation/Cherenkov material. Radioluminescence (RL) spectra of 0.01% Pr-doped PWO reported in Ref. 15 display the Pr³⁺ 4*f*-4*f* lines within 480–650 nm with decay times of units to tens of microseconds. Heavy Pr³⁺ doping could in principle provide the same damping effect on (here undesired) nanosecond PWO intrinsic luminescence as seen for La doping.¹⁰ Besides, the Pr³⁺ 4*f*-4*f* emission lines in the red spectral region contribute to the scintillation output, and their intensity and decay time could be further tuned by the concentration quenching effect. Hence, in the

^{a)}Author to whom correspondence should be addressed. Electronic mail: nikl@fzu.cz.

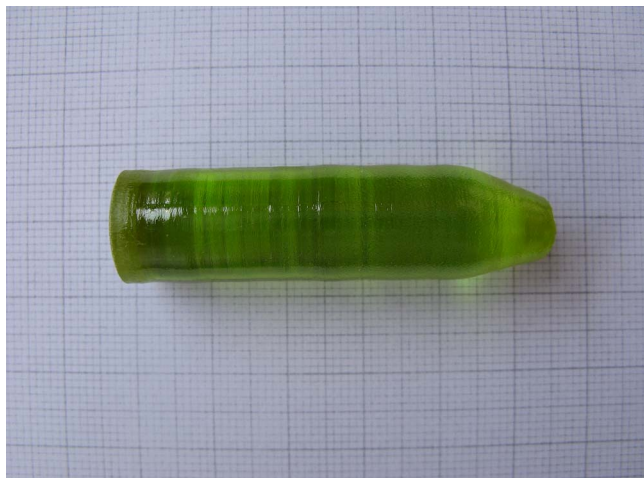


FIG. 1. (Color online) Photograph of the as grown 5%Pr:PbWO₄ crystal.

present study we report the preparation and characterization of Pr-doped single crystals in a wide concentration range (0.1–5 mol %).

II. EXPERIMENTAL CONDITIONS

Three Pr-doped PWO single crystals with a diameter of 13 mm and length about 50 mm were grown by Czochralski technique using PbO and WO₃ raw powders with a purity of 5N and 4N, respectively. Starting contents of Pr₆O₁₁ in the melt were 0.1, 1.0, and 5.0 mol % and in the following the crystals will be correspondingly referred to as 0.1%Pr, 1%Pr, and 5%Pr. In the first two cases PbO concentration was kept at 49.5 mol %, while in the case of the highest Pr doping it had to be decreased to 46.9 mol % to obtain a transparent and crack-free crystal (see Fig. 1). Optical elements (30 mm long cylinder and 1 mm thick plates) were cut from the parent boule and polished to an optical grade.

Optical absorption was measured at room temperature (RT) using a Shimadzu absorption spectrometer UV-3101PC. RL (excitation by an x-ray tube operated at 40 kV) was measured by an upgraded spectrofluorometer 199S (Edinburgh Instrument) with the TBX-04 (IBH Scotland) photon counting fast photomultiplier-based detector. Steady-state photoluminescence spectra were measured using a hydrogen lamp for the excitation in the same setup used for RL. The emission spectra were corrected for the spectral sensitivity of the detection part (single grating monochromator and Philips XP2233 photomultiplier), while the excitation spectra were corrected for the spectral dependence of the excitation energy, which is given by the hydrogen lamp spectrum and characteristics of the single-grating-excitation monochromator. Photoluminescence decays excited in the UV/visible spectral region were measured using a microsecond xenon flash lamp (pulse full width at half maximum of about 2 μs) typically with a 10 Hz repetition frequency. The detection was performed by the mentioned TBX-04 module and multichannel analyzer working in the scaling mode with a time resolution of 500 ns/channel. A deconvolution procedure was applied to extract true decay times. All measurements were performed at RT.

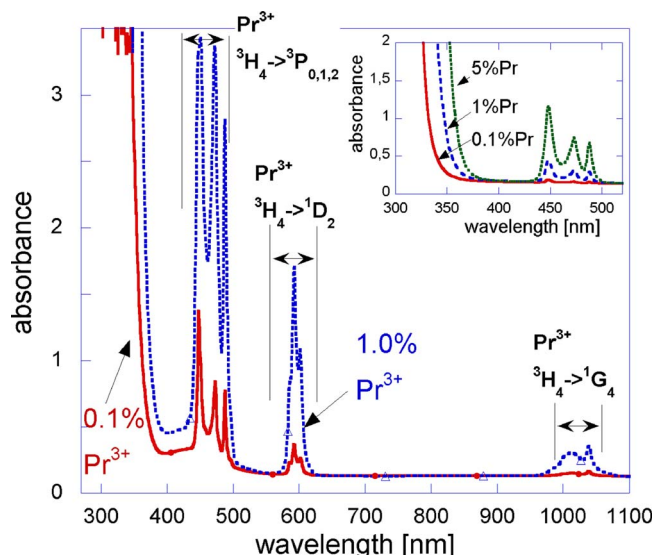


FIG. 2. (Color online) Absorption spectra of Pr³⁺-doped PWO (0.1%Pr and 1%Pr) measured on 30 mm long cylinders. The inset provides an enlargement including the sample absorption edge and the ${}^3H_4\text{-}{}^3P_{2,1,0}$ transitions of Pr³⁺ for the 0.1%–1.0%–5%Pr concentrations measured on 1 mm thick plates.

Thermally stimulated luminescence (TSL) measurements after x-ray irradiation (by a Machlett OEG 50 x-ray tube operated at 20 kV) at RT were performed from RT up to 400 °C with a linear heating rate of 1 °C/s. The total emitted light was detected as a function of temperature in the photon counting mode using an EMI 9635 QB photomultiplier tube.

III. EXPERIMENTAL RESULTS

Absorption spectra with marked $4f\text{-}4f$ absorption transitions of Pr³⁺ ion are displayed in Fig. 2. Excellent transparency of the 30 mm long crystal cylinders outside of Pr³⁺-related absorption transitions is evident. It is interesting to note that Pr³⁺ doping results in a noticeable low energy shift of the PbWO₄ absorption edge (in the undoped crystal it occurs at about 325 nm at RT). The shift increases with increasing Pr concentration.

Photoluminescence spectra in Fig. 3 show the $4f\text{-}4f$ emission lines of Pr³⁺ starting from the 3P_0 and 1D_2 levels and ending at the 3H_x ground state or 3F_x multiplets (see assignment in Fig. 4). Excitation spectra indicate that aside from exciting the Pr³⁺ emission directly into the Pr³⁺ levels (${}^3P_{1,2}$ levels of Pr³⁺ around 450 nm), one can also excite it via the host (at wavelengths shorter than about 315 nm) and below the host exciton absorption at about 325 nm. RL spectra are displayed in Fig. 4. They are consistent with the emission spectra reported in Fig. 3. It is worth noting the intensity decrease in PWO host emission with increasing Pr concentration. The intrinsic emission of PbWO₄ is practically absent already at 1%Pr concentration.

Photoluminescence decay of the dominant 645 nm emission line of the 1%Pr sample is shown in Fig. 5. The decay is a single exponential with the decay time of about 2 μs. Shortening of decay times of the 645 nm (starting from 3P_0) and 610 nm (starting from 1D_2) radiative transitions with

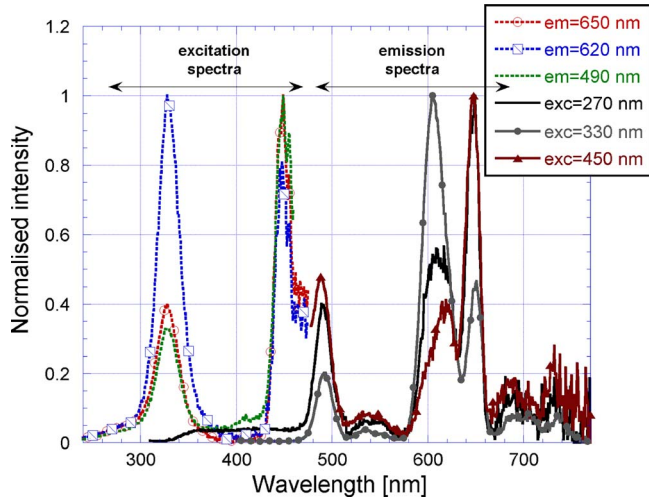


FIG. 3. (Color online) Excitation (at $\lambda_{em}=650, 620,$ and 490 nm) and emission (at $\lambda_{exc}=270, 330, 450$ nm) spectra of 1%Pr crystal measured on a 1 mm thick plate.

increasing Pr concentration (see the inset) can be explained by concentration quenching as it is accompanied by emission intensity decrease (Fig. 4).

The spectrally unresolved scintillation decay of the 1%Pr sample is shown in Fig. 6. More than 90% of the scintillation intensity is released in the 1940 ns component, which coincides with the dominant photoluminescence decay time of Pr^{3+} .

TSL glow curves above RT, in Fig. 7, are dominated by well-known peaks¹⁶ at about 60–70 °C followed by a high T shoulder at about 150 °C in the case of 0.1%Pr and 1%Pr samples, while in the case of the 5%Pr sample the TSL signal is practically absent at any temperature. Considerably strong decrease in the TSL intensity with increasing Pr concentration (much more significant than that of RL intensity) points to suppression of deep electron traps based on oxygen

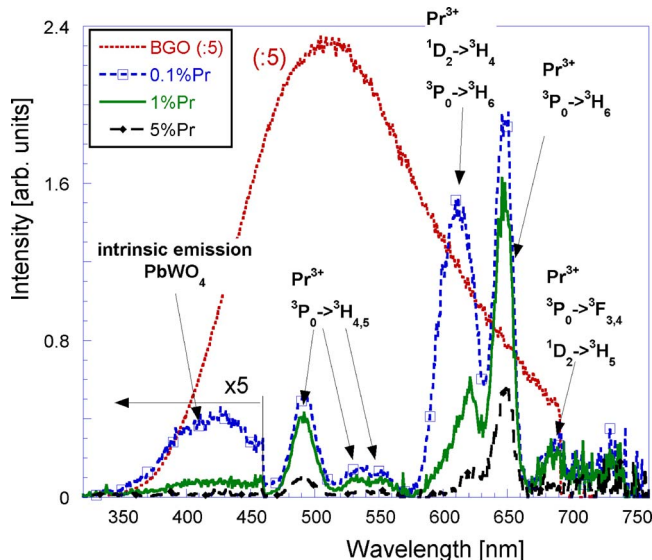


FIG. 4. (Color online) RL spectra of three PWO:Pr crystals in quantitative comparison with that of a BGO standard scintillator (equally shaped samples, 1 mm thick plates).

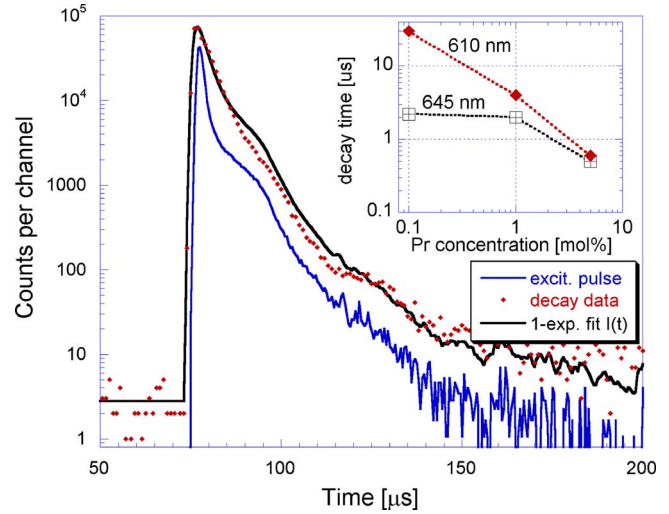


FIG. 5. (Color online) Photoluminescence decay of 1%Pr sample, $\lambda_{exc}=330$ nm, $\lambda_{em}=650$ nm. The thick solid line is the convolution of the instrumental response (measured excitation pulse) and of the function $I(t) = 74\,428 \exp(-t/1.97 \mu s) + 2.79$. The inset shows the Pr-concentration dependence of the decay time in the 610 and 645 nm emission lines.

vacancies in the host and is consistent with a positive role of trivalent dopants in the PWO structure as mentioned earlier.^{17,18}

IV. DISCUSSION

All Pr-doped samples show the Pr^{3+} 4f-4f emission lines in the green-red part of the spectra in agreement with previous results.¹⁵ The PWO host emission is progressively suppressed with increasing Pr^{3+} concentration similar to what is observed for heavy doping by other trivalent ions such as La^{3+} and Gd^{3+} .^{10,19} The concentration quenching of 4f-4f emission with increasing Pr^{3+} concentration is clearly evidenced already between 0.1%–1% and above 1% in the case of transitions from 1D_2 and 3P_0 levels, respectively. Due to this effect the photoluminescence decay times are shortened to about 500 ns in the case of 5%Pr doping, while the scintillation intensity is accordingly reduced. In the 1%Pr crystal the scintillation decay is governed by the decay time compo-

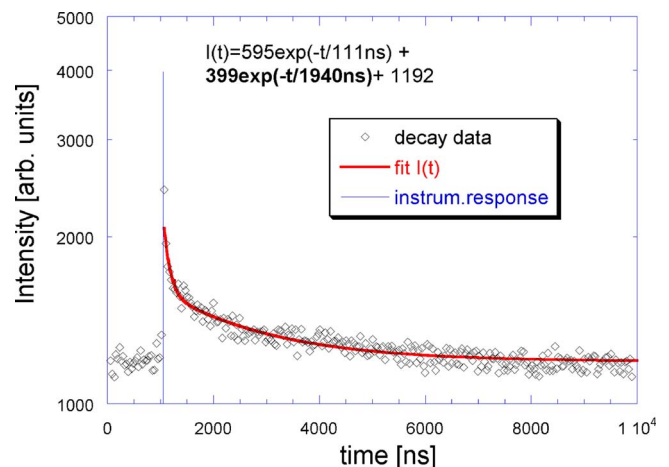


FIG. 6. (Color online) Spectrally unresolved scintillation decay of 1%Pr sample (30 mm long cylinder, excited by 511 keV photons of ^{22}Na radioisotope).

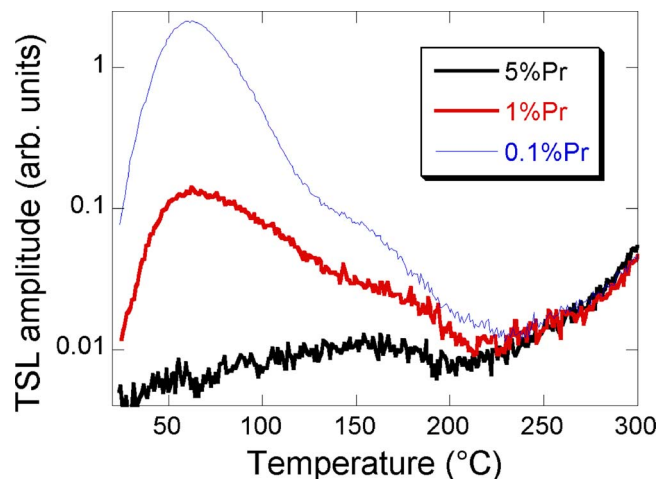


FIG. 7. (Color online) TSL glow curves of all PWO:Pr samples after x-ray irradiation at RT. The signal increase above 230 °C is due to black body radiation of the TSL heater.

ment identical to that of the 3P_0 - 3H_6 photoluminescence line at 645 nm so that no additional delays have been observed due to energy transfer from the host. The suppression of TSL intensity at higher Pr concentration is consistent with the effect of other trivalent dopants as mentioned earlier. The TSL spectrum shows Pr^{3+} $4f$ - $4f$ lines together with other components possibly associated with defects. However, the weak TSL intensity of the samples does not allow its detailed analysis. Nevertheless, it can be concluded that the TSL mechanism above RT consists in the liberation of electrons from deep electron traps due to oxygen vacancies¹⁸ and their radiative recombination with the holes trapped at intrinsic defects and Pr^{3+} ions.²⁰

An interesting question arises about the nature of the low energy shift of the absorption edge of the host from 330 to 350 nm and about the mechanism of excitation of the Pr^{3+} $4f$ - $4f$ luminescence in this spectral region. In principle one can consider either transition from the Pr^{3+} 3H_4 ground state to the conduction band or a charge transfer transition from oxygen ligands toward Pr^{3+} (i.e., a temporary creation of Pr^{2+} bound to a hole at oxygen ligands) as possible processes responsible for the low energy shift of the absorption edge. Considering the first hypothesis, we note that in Ce^{3+} -doped PWO, such a low energy shift should be about 1.5 eV higher with respect to Pr-doping due to the mutual positions of the Ce^{3+} and Pr^{3+} ground states in the forbidden gap of dielectric compounds.²¹ Hence, a shift in the absorption edge to approximately 600–650 nm should be observed, while Ce-doped PWO shows the absorption edge in the near UV.^{10,19} In contrast, the stable appearance of Pr^{2+} in oxide compounds is not excluded and its energy position is expected to be rather close to the conduction band.²¹ Therefore, we tentatively associate the observed low energy shift of the absorption edge in PWO:Pr to the charge transfer transition from oxygen ligands toward Pr^{3+} ions. Alternatively, one could explain the low energy shift of the absorption edge merely due to a perturbation introduced by the rare earth (RE) trivalent ion on the fundamental exciton absorption transition in the PWO structure as this effect is also observed in heavily La- or Gd-doped PWO (Ref. 10) where the above

suggested charge transfer transition can be hardly supposed. However, in the case of the latter dopings the magnitude of the absorption edge shift is smaller than that here detected; interestingly, it is similar to the depth of the $(\text{WO}_4)^{3-}$ - La^{3+} electron trap.¹⁷ Consequently, it could also be proposed that the observed shift is due to a sort of charge transfer transition between oxygen ligands and $(\text{WO}_4)^{2-}$ - RE^{3+} centers. Ligand-to-metal charge transfer absorption transition is currently observed in Yb-doped compounds and is followed by both charge transfer and $4f$ - $4f$ luminescence of Yb^{3+} ions.²² The charge transfer luminescence of Pr^{3+} can easily be quenched due to supposed vicinity of the charge transfer and 3P_0 levels so that only $4f$ - $4f$ emission can be detected, as it really occurs.

The heavy doping of Pr^{3+} into the PWO lattice is technologically feasible up to, at least, several percent. It provides a tool for tuning the scintillation intensity within the green-red spectral region from a few percent of BGO standard scintillator down to a fraction of percent in the studied concentration range. The scintillation response is governed by decay times in the 100–2000 ns interval. Due to excellent spectral and temporal resolutions between the Cherenkov and scintillation components, which are moreover expected of comparable intensity, heavily Pr-doped PWO appears very favorable for the application of this material for dual scintillation/Cherenkov light detector under the assumption that Cherenkov light will not be too attenuated due to the described low energy shift of the host absorption edge and the 3H_4 - ${}^3P_{2,1,0}$ absorption transition of Pr^{3+} in the 450–490 nm range.

V. CONCLUSIONS

Pr-doping of PWO single crystals results in the appearance of typical $4f$ - $4f$ absorption and luminescence transitions of Pr^{3+} in the green-red part of the spectrum. RL spectra manifest considerable reduction in the host blue luminescence with increasing Pr^{3+} concentration. The major part of Pr^{3+} emission intensity is released with a decay time of about 2 μs in the sample with the lowest dopant concentration and the decay time becomes shorter for Pr concentration above 1%. Concentration quenching is thus evidenced from the decrease in decay times related to transitions from both 1D_2 and 3P_0 levels of Pr^{3+} . The overall scintillation efficiency can be estimated by the integrated RL spectra of 1%Pr and 5%Pr samples, which are about 3% and 0.5% of that of BGO, respectively. Due to the small Stokes shift the emission lines at 490 and 610 nm will be noticeably reabsorbed in the bulk elements and high Pr concentrations, while there is no reabsorption problem for the dominant 3P_0 - 3H_6 emission line at about 645 nm. The principal scintillation decay time in Pr1% sample coincides with that of photoluminescence. Another minor (5%–10% of intensity) component of about 110 ns decay time was also detected; however, its origin is not clear. The low energy shift of the absorption edge in the near UV is tentatively assigned to the oxygen ligand $\rightarrow \text{Pr}^{3+}$ [$(\text{WO}_4)^{2-}$ - Pr^{3+}] charge transfer transition and/or to perturbation of exciton absorption transition due to the presence of trivalent ions in the lattice.

ACKNOWLEDGMENTS

This research was supported by Czech Institutional Research Plan No. AV0Z10100521 and GA AV No. IAA100100810 projects. Thanks is due to E. Mihokova for linguistic corrections.

- ¹(a) W. van Loo, *Phys. Status Solidi A* **27**, 565 (1975); (b) W. van Loo, *ibid.* **28**, 227 (1975).
- ²J. A. Groenink and G. Blasse, *J. Solid State Chem.* **32**, 9 (1980).
- ³R. Oeder, A. Scharmann, D. Schwabe, and B. Vit, *J. Cryst. Growth* **43**, 537 (1978).
- ⁴V. G. Baryshevsky, M. V. Korzhik, V. I. Moroz, V. B. Pavlenko, A. S. Lobko, A. A. Fyodorov, V. A. Kachanov, V. L. Solovjanov, B. I. Zadneprovsky, V. A. Nefyodov, P. V. Nefyodov, B. A. Dorogovin, and L. L. Nagornaja, *Nucl. Instrum. Methods Phys. Res. A* **322**, 231 (1992).
- ⁵M. Kobayashi, M. Ishii, Y. Usuki, and H. Yahagi, *Nucl. Instrum. Methods Phys. Res. A* **333**, 429 (1993).
- ⁶S. Baccaro, P. Boháček, B. Borgia, A. Cecilia, I. Dafinei, M. Diemoz, M. Ishii, O. Jarolimek, M. Kobayashi, M. Martini, M. Montecchi, M. Nikl, K. Nitsch, Y. Usuki, and A. Vedda, *Phys. Status Solidi A* **160**, R5 (1997).
- ⁷M. Kobayashi, Y. Usuki, M. Ishii, T. Yazawa, K. Hara, M. Tanaka, M. Nikl, and K. Nitsch, *Nucl. Instrum. Methods Phys. Res. A* **399**, 261 (1997).
- ⁸M. Nikl, *Phys. Status Solidi A* **178**, 595 (2000).
- ⁹A. Annenkov, M. V. Korzhik, and P. Lecoq, *Nucl. Instrum. Methods Phys. Res. A* **490**, 30 (2002).
- ¹⁰M. Kobayashi, S. Sugimoto, Y. Yoshimura, Y. Usuki, M. Ishii, N. Sengutuvan, K. Tanji, and M. Nikl, *Nucl. Instrum. Methods Phys. Res. A* **459**, 482 (2001).
- ¹¹Y. L. Huang, W. L. Zhu, X. Q. Feng, and Z. Y. Man, *J. Solid State Chem.* **172**, 188 (2003).
- ¹²W. Li, X. Q. Feng, and Y. Huang, *J. Phys.: Condens. Matter* **16**, 1325 (2004).
- ¹³T. Chen, T. Y. Liu, Q. R. Zhang, F. F. Li, D. S. Tian, and X. Y. Zhang, *Phys. Lett. A* **363**, 477 (2007).
- ¹⁴(a) R. Wigmans, *Nucl. Instrum. Methods Phys. Res. A* **572**, 215 (2007); (b) N. Akchurin, L. Berntzon, A. Cardini, R. Ferrari, G. Gaudio, J. Hauptman, H. Kim, L. La Rotonda, M. Livan, E. Meoni, H. Paar, A. Penzo, D. Pinci, A. Policicchio, S. Popescu, G. Susinno, Y. Roh, W. Vandelli, and R. Wigmans, *ibid.* **582**, 474 (2007); (c) N. Akchurin, A. Astwood, A. Cardini, G. Ciapetti, R. Ferrari, S. Franchino, M. Fraternali, G. Gaudio, J. Hauptman, F. Lacava, L. La Rotonda, M. Livan, E. Meoni, H. Paar, D. Pinci, A. Policicchio, S. Popescu, G. Susinno, Y. Roh, W. Vandelli, *et al.*, "Separation of crystal signals into scintillation and Cherenkov components," *ibid.* **595**, 359 (2008).
- ¹⁵M. Nikl, P. Boháček, E. Mihoková, N. Solovieva, M. Martini, A. Vedda, P. Fabeni, G. P. Pazzi, M. Kobayashi, M. Ishii, Y. Usuki, and D. Zimmerman, *J. Cryst. Growth* **229**, 312 (2001).
- ¹⁶M. Nikl, K. Nitsch, S. Baccaro, A. Cecilia, M. Montecchi, B. Borgia, I. Dafinei, M. Diemoz, M. Martini, E. Rosetta, G. Spinolo, A. Vedda, M. Kobayashi, M. Ishii, Y. Usuki, O. Jarolimek, and R. Uecker, *J. Appl. Phys.* **82**, 5758 (1997).
- ¹⁷V. V. Laguta, M. Martini, F. Meinardi, A. Vedda, A. Hofstatter, B. K. Mayer, M. Nikl, E. Mihokova, J. Rosa, and Y. Usuki, *Phys. Rev. B* **62**, 10109 (2000).
- ¹⁸V. V. Laguta, M. Martini, A. Vedda, E. Rosetta, M. Nikl, E. Mihokova, J. Rosa, and Y. Usuki, *Phys. Rev. B* **67**, 205102 (2003).
- ¹⁹M. Nikl, P. Boháček, E. Mihoková, J. Rosa, M. Martini, A. Vedda, P. Febeni, G. P. Pazzi, V. Laguta, M. Kobayashi, M. Ishii, Y. Usuki, D. Zimmerman, S. Baccaro, and A. Cecilia, *Radiat. Meas.* **33**, 705 (2001).
- ²⁰M. Nikl, A. Vedda, and V. V. Laguta, *Radiat. Meas.* **42**, 509 (2007).
- ²¹P. Dorenbos, *J. Phys.: Condens. Matter* **15**, 8417 (2003).
- ²²L. van Pieterse, M. Heeroma, E. de Heer, and A. Meijerink, *J. Lumin.* **91**, 177 (2000).